

archives  
of thermodynamics

Vol. 41(2020), No. 2, 169–184  
DOI: 10.24425/ather.2020.133627

## Neuro-genetic optimization of ribbed heat exchanger using entropy augmentation generation number

PAVAN K. KONCHADA<sup>\*a</sup>  
BHATTI SUKHVINDER<sup>b</sup>  
SIDDHARDHA RELANGI<sup>c</sup>  
RAMBHADRIRAJU CHEKURI<sup>d</sup>

<sup>a</sup> Mahatma Gandhi Institute of Technology, Gandipet, Hyderabad, Telangana 500075, India

<sup>b</sup> Andhra University, Visakhapatnam 530003, Andhra Pradesh, India

<sup>c</sup> Gayatri Vidya Parishad School of Engineering, Visakhapatnam, Andhra Pradesh, 530048, India

<sup>d</sup> SRKR College of Engineering, Chinnaamiram, 534204 Bhimavaram, India

**Abstract** Numerical predictions of heat transfer under laminar conditions in a square duct with ribs are presented in this paper. Ribs are provided on top and bottom walls in a square duct in a staggered manner. The flow rates have been varied between Reynolds number 200 and 600. Various configurations of ribs by varying length, width and depth have been investigated for their effect on heat transfer, friction factor and entropy augmentation generation number. Further artificial neural network integrated with genetic algorithm was used to minimize the entropy augmentation generation number (performance factor) by selecting the optimum rib dimensions in a selected range. Genetic algorithm is compared with microgenetic algorithm to examine the reduction in computational time for outlay of solution accuracy.

**Keywords:** Rib; Square duct; Entropy augmentation generation number; Artificial neural network; Micro genetic algorithm

---

\*Corresponding Author. Email: pavankonchada@gmail.com

## Nomenclature

$i, j$	– indices (= 1, 2, 3)
$k$	– thermal conductivity, W/mK
$L, W, D$	– length, width, depth, m
$N_{s,a}$	– entropy augmentation generation number
$Nu$	– Nusselt number
$P$	– pressure, Pa
$Re$	– Reynolds number
$\dot{s}_{gen}$	– local entropy generation (W/m <sup>3</sup> K)
$\dot{S}_{gen}$	– global entropy generation (W/K)
$\dot{S}_{gen,o}$	– original global entropy generation, W/K
$\dot{S}_{gen,a}$	– augmented global entropy generation, W/K
$T$	– temperature, K
$t_{ANN,i}$	– neural network output
$t_{num,i}$	– actual output
$u_i$	– velocity components, m/s
$x_j$	– Cartesian coordinates, m

## Greek symbols

$\alpha$	– thermal diffusivity, m <sup>2</sup> /s
$\nu$	– kinematic viscosity, m <sup>2</sup> /s
$\rho$	– density of fluid, kg/m <sup>3</sup>
$\phi$	– viscous dissipation rate, W/ m <sup>3</sup>

## Abbreviations

ANN	– artificial neural network
GA	– genetic algorithm
$\mu$ GA	– microgenetic algorithm

## 1 Introduction

Compact heat exchangers are being developed due to the space constraint. The thermal performance of a heat exchanger is strongly influenced by the thermal resistance between the fluids. It includes the conductive resistance of tube material and the convective resistance due to the static boundary layer of the fluid over the tube wall. Stagnation boundary layer formed is major cause for decreasing heat transfer rates. Turbulators like the rib roughened tubes, twisted tape inserts, and conical ring inserts, etc. play a major role for enhancement of convective heat transfer. These techniques induce a disturbance in the boundary layer flow, which promotes the fluid mixing and thereby increases the heat transfer rate at moderate cost of pumping power.

Thianpong *et al.* [1] have reported the effect in case of water as the working fluid of a dimpled tube fitted with a twisted tape insert on heat transfer and friction. The results show that the twisted tape inserted dimpled tube has higher friction factor and convective heat transfer coefficient than those of a dimpled tube and a smooth tube. Kathait and Patil [2] investigated the effect of discrete corrugated rib roughness on heat transfer and frictional losses in a heat exchanger tube. It brought out 2.73 and 2.78 folds enhancements in the Nusselt number and friction factor, respectively for corrugated tube with five numbers of gaps. Kamali and Binesh [3] studied friction and heat transfer with various-shaped ribs mounted on one wall in a square duct. The simulations were performed with decreasing height in the flow direction for four rib shapes, i.e., square, triangular, trapezoidal, and with increasing height in the flow direction for trapezoidal. The results show that the heat transfer coefficients were strongly affected by the rib shape. Trapezoidal ribs with decreasing height in the flow direction provide higher heat transfer enhancement and pressure drop. Jaurker *et al.* [4] stated that Nusselt number can be further enhanced beyond that of ribbed duct while keeping the friction factor enhancement low with rib-grooved artificial roughness on one broad heated wall of a large aspect ratio duct. Thinapong *et al.* [5] presented an experimental investigation on turbulent heat transfer and friction loss behaviors of airflow through a constant heat flux channel fitted with different heights of triangular ribs. Webb *et al.* [6] experimentally studied the effect of different rib spacing, rib height and rib angles on the heat exchanger performance in circular tubes having a repeated-rib roughness. Manca *et al.* [7] presented a numerical investigation with a constant heat flux applied on the bottom and upper external walls on forced convection in a rectangular channel with air as medium. Thinapong *et al.* [8] presented the influence of different heights of triangular ribs on turbulent heat transfer and friction loss behaviors of airflow through a constant heat flux channel fitted with experimentally. Skullong *et al.* [9] had investigated the heat transfer in heat exchanger at the rib angle of  $45^\circ$  for varying rib height to channel height ratios (0.1, 0.15, 0.2). Choi *et al.* [10] has compared the heat transfer coefficient for varying dimple diameters, dimple pitch, rib pitch and rib angle. Liu *et al.* [11] had investigated the effect of cylindrical ribs in a square duct on heat transfer. Abed *et al.* [12] presented a computational study flow characteristics and heat transfer in corrugated with V-shape lower plate using nano fluids. The computations are performed uniform heat flux over a range of

Reynolds number  $Re = 8000\text{--}20\,000$ . V-shaped wavy channels proved to be advantages by using nano fluids and thus serve as promising candidates. Piechowski based on the second law of thermodynamics studied a relatively new approach to optimisation of a ground heat exchanger. He worked to get optimum combination of circulating water flow rate and pipe diameter [13]. Bejan [14–17] showed entropy is generated through temperature gradient and fluid friction in a heat exchanger. Sekulic *et al.* [18] using enthalpy exchange irreversibility norm discussed the behavior of parallel flow and counter flow heat exchangers. Sekulic *et al.*[19] further using the entropy generation estimated the quality of the heat exchange process in heat exchanger. Ogulata *et al.* [20] experimentally studied cross flow plate-type heat exchanger using entropy generation number. Laskowski estimated the diameter of church window condenser using entropy generation minimization approach [21]. Konchada *et al.* [22] had taken entropy generation as measuring parameter of heat exchanger efficiency, and analyzed the effect of mass flow and other parameters on entropy generation. New optimization technique by combining artificial neural networks (ANN) and genetic algorithms (GA) was proposed and applied to natural convection by Kadiyala and Chattopadhyay [23]. Optimum set of parameters are found to maximize the heat transfer rate for laminar slot jets impinging on the surface using ANN combined with GA by Kadiyala and Chattopadhyay [24]. Li *et al.* [25] had combined ANN with a multi-objective genetic algorithm (MOGA) to maximize the heat transfer and minimize the pressure drop for given corrugation height and angle of attack as input parameters. Ge *et al.* [26] had optimized six microchannel parameters using multi-objective genetic algorithm and multi-objective particle swarm optimization to maximize the heat transfer, Kishore *et al.* [27] had estimated the optimum dimple position, diameter and pitch of twisted tape by ANN combined with GA to find the maximum thermohydraulic performance factor.

From the above literature study it is clear that no work has been done to augment the heat transfer rate by varying all the rib parameters (length, width, and height) placed alternatively on top and bottom surface of duct. In this present study so computational fluid dynamics analysis is carried using commercial code Fluent on square ducts with rectangular ribs of different dimensions with water as working fluid. The ribs are positioned alternatively on top and bottom of duct to boost the fluid mixing. Periodic boundary condition was imposed on inlet and outlet to simulate it as fully developed flow. Then entropy generation number was calculated for

different configuration and Reynolds number. Optimization technique GA integrated with ANN was used to obtain the optimal solution for the given rib dimensions.

## 2 Numerical procedure

### 2.1 Mathematical model

A square duct of 13 mm side and length 156 mm is considered adopted from works of Saha and Mallik [28]. Rectangular ribs of depth 2–3 mm, length 8–9 mm, and width 2–4 mm are considered on the duct alternatively on top and bottom of duct as shown in Fig. 1.

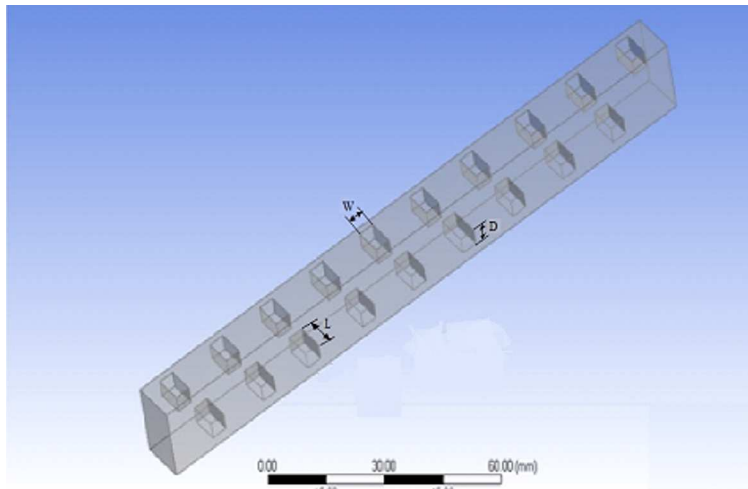


Figure 1: Model of square duct with rectangular ribs.

### 2.2 Governing equations

The conservation equations representing steady state continuity, momentum and energy neglecting compressibility and viscous dissipation are given below, using index notation ( $i, j = 1, 2, 3$ ):

continuity equation

$$\frac{\partial u_i}{\partial x_i} = 0, \quad (1)$$

momentum equation

$$u_j \frac{\partial u_i}{\partial x_j} = -\frac{1}{\rho} \frac{\partial P}{\partial x_i} + \nu \frac{\partial^2 u_i}{\partial x_j \partial x_j}, \quad (2)$$

energy equation

$$u_j \frac{\partial T}{\partial x_j} = \alpha \frac{\partial^2 T}{\partial x_j \partial x_j}. \quad (3)$$

### 2.3 Mesh independence study and validation

Mesh independence study is carried out for ribbed duct with unstructured mesh and heat transfer coefficient as output parameter. The selected mesh with 689 954 elements has deviated 0.9% from previous 532 756 elements step by following Richardson extrapolation (Fig. 2). And hence above considered mesh configuration is used in further simulations. Mesh with proximity, curvature and inflation turned on for simulation as shown in Fig. 3.

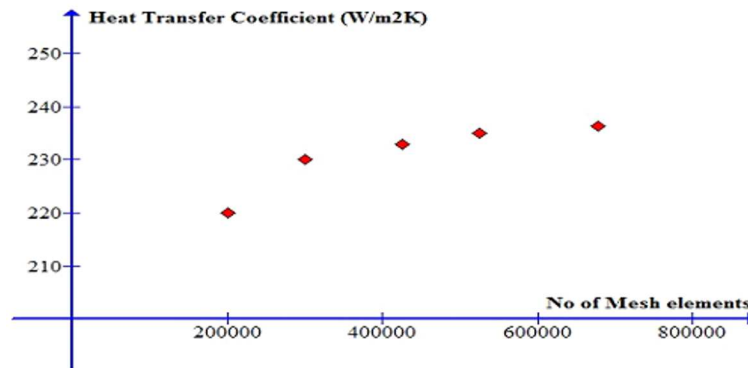


Figure 2: Mesh independence study.

### 2.4 Boundary conditions and solution procedure

A constant heat flux of 10 000 W/m<sup>2</sup> was applied on the wall of ribbed duct and a no slip boundary condition. The inlet and outlet of the ribbed duct are assumed periodic to interpret the flow as fully developed.

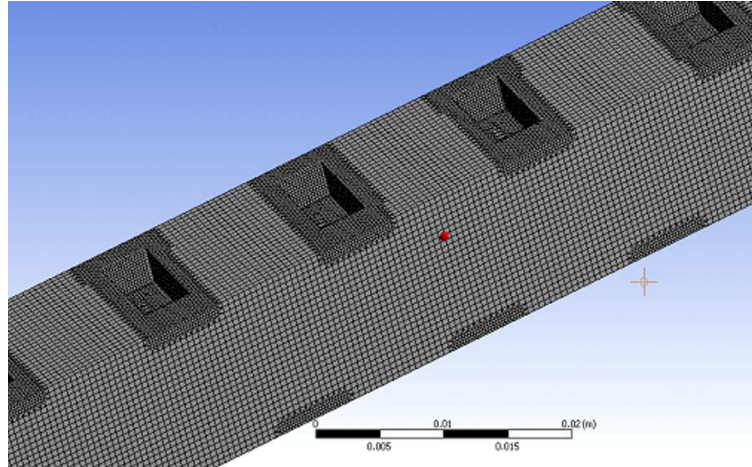


Figure 3: Mesh of square duct with rectangular ribs.

The semi implicit pressure linked equation (SIMPLE) algorithm was used for pressure-velocity coupling. Second order scheme is used for momentum, energy and pressure for spatial discretization. The convergence criteria set for equations of momentum and continuity is  $10^{-4}$  and for energy is  $10^{-7}$ .

## 2.5 Entropy augmentation generation number

Entropy generation rate consists of two parts one ‘viscous’ ( $\dot{s}_v$ ), depends on the physical viscosity, on the local temperature of the fluid and on the second power of the local velocity gradient, and another, called ‘thermal’ ( $\dot{s}_T$ ), that depends on the physical conductivity, square of the local temperature of the fluid and second power of the local temperature gradient:

$$\dot{s}_{gen} = \dot{s}_T + \dot{s}_v = \frac{k}{T^2} \left[ \left( \frac{\partial T}{\partial x_1} \right)^2 + \left( \frac{\partial T}{\partial x_2} \right)^2 + \left( \frac{\partial T}{\partial x_3} \right)^2 \right] + \frac{\phi}{T}, \quad (4)$$

whereas  $\phi$  being the rate of viscous dissipation per unit volume. In our case flow considered is laminar so the viscous dissipation is neglected. Note that the entropy generation rate expressed in (4) is per unit volume ( $\text{W}/\text{m}^3\text{K}$ ). The global entropy generation rate of the entire domain is computed as the integral of the local rates

$$\dot{S}_{gen} = \int_v \dot{s}_{gen} dv. \quad (5)$$

Thermodynamic impact of augmented case can be compared to the original one. Bejan and Pfister [29] proposed that the merit of a given heat transfer augmentation technique may be evaluated by comparing the rate of entropy generation of the heat exchange apparatus before and after the implementation of the augmentation technique. Entropy generation augmentation number is given by [30–32]

$$N_{s,a} = \frac{\dot{S}_{gen,a}}{\dot{S}_{gen,o}}. \quad (6)$$

For  $N_{s,a} < 1$  are thermodynamically advantageous augmentation technique because, in addition to enhancing heat transfer, they reduce the degree of irreversibility of the apparatus.

### 3 Outline of optimization

#### 3.1 Genetic algorithm

Genetic algorithms (GA) are adaptive heuristic search algorithms premised on the evolutionary ideas of natural selection and genetic [33]. These algorithms encode a potential solution to a specific problem on a simple chromosome-like data structure and apply genetic operators to these structures [34]. The flow chart for optimization was given by Kadiyala and Chattopadhyay [23]. Population size and the crossover fraction considered is 20 and 0.8.

#### 3.2 Microgenetic algorithm

The microgenetic algorithm ( $\mu$ GA) is a small population genetic algorithm. Computational time required to achieve best fit solution is less due to size of population. The population size is 5 for each generation. The flow diagram was given by Madadi and Balaji [35].

#### 3.3 Artificial neural network (back propagation)

One of the ANN models extensively used for power system application is the multilayer perceptron model based on the back propagation algorithm [23,27].

## 4 Results and discussions

Numerical simulation procedure adopted in this study is compared with the numerical results obtained by Nonino and Comini for  $90^\circ$  staggered ribs in a square duct [36]. There is a maximum of 3% variation obtained by the adopted procedure compared to Nonino results. Present solution procedure is also applied to plain square duct has given a maximum variation of 6% (fully developed flow) compared to a known value of 3.63.

### 4.1 Heat transfer

The enhancement of heat transfer rate can be observed in Fig. 4 compared to a plain square duct due to increase in mixing of flow and flow rotation. The fluid starts reattaching the surface after the rib and thus helping to

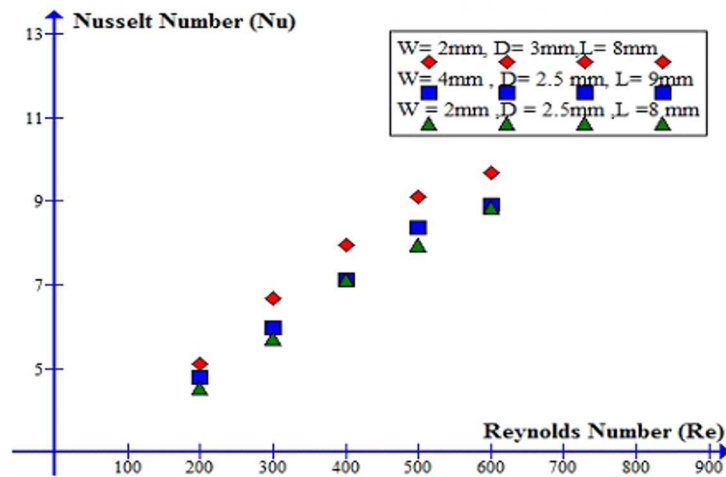


Figure 4: Nusselt number versus Reynolds number for ribbed duct.

mixing of fluid rigorously and increasing thermal dispersion. Rate of increase in heat transfer rate decreases (Nusselt number,  $Nu = 5.1$  increases to 6.6 and  $Nu = 9.11$  to 9.7, respectively) as the Reynolds number augments due to the decrease in thermal capacity of fluid. The local maxima heat transfer coefficient will be in the spacing of ribs due to reattaching flow and hence heat transfer coefficient would be more in the space between two ribs. The augmentation is mostly depending on the depth of rib compared to width and length due to contact area improvement.

## 4.2 Friction factor

It can be noted that from Fig. 5 friction factor increases with the depth of rib due to escalation in local stagnation area. At high Reynolds number the friction factor is low for any dimension of rib but at low Reynolds number friction factor was high for any configuration, since at high Reynolds number inertia dominates the viscous forces for the given configuration. The variation of friction factor at low Reynolds number is approximately 40% compared to high Reynolds number 16% due to velocity of flow.

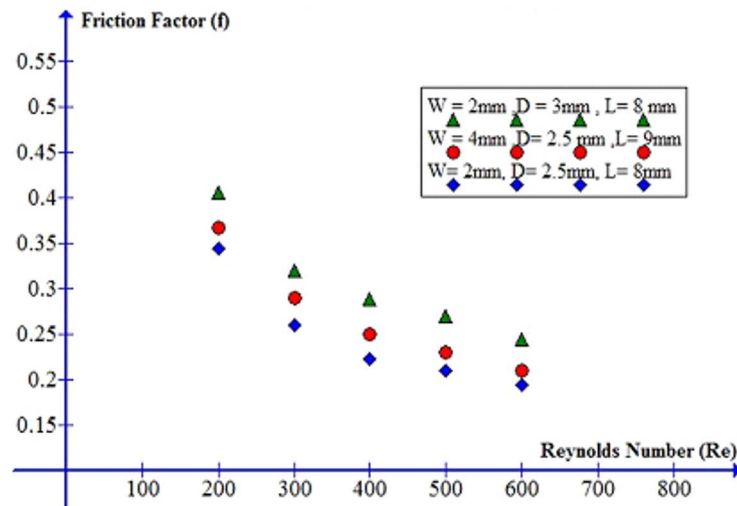


Figure 5: Friction factor versus Reynolds number for ribbed duct.

## 4.3 Entropy generation augmentation number

Entropy augmentation generation number is lower at high Reynolds number due to low thermal gradients compared to low Reynolds number. From Fig. 6 it can be inferred that as the depth increases heat transfer rate is increased correspondingly  $N_{s,a}$  is decreased, and hence we can consider  $N_{s,a}$  as performance criteria for heat exchanger.

In Matlab software a feed forward back propagation network is used which is trained by using the Levenberg-Marquardt algorithm which is also used in the least squares curve fitting problem [27]. The inputs to the ANN are the length ( $L$ ), width ( $W$ ) and depth ( $D$ ) of the rib and the required

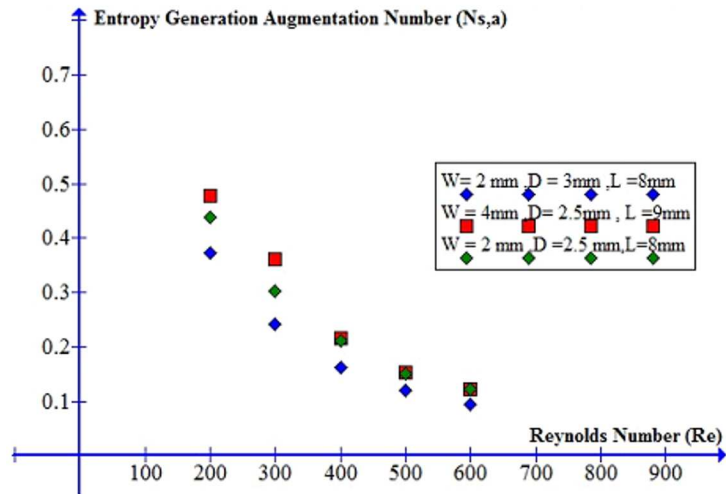


Figure 6: Entropy generation augmentation number versus Reynolds number.

output is entropy augmentation generation number. The input parameters are varied according to different sizes in which the depth is varying from 2 mm to 3 mm, the width of the rib varying from 2 mm to 4 mm and the length of the rib varying from 8 mm to 9 mm. Number of neurons in the hidden layer was selected by using performance parameter such as the root mean square error (RMSE). The parameter is defined as

$$\text{RMSE} = \sqrt{\frac{\sum_{i=1}^N (t_{ANN,i} - t_{num,i})^2}{N}} \quad (7)$$

where  $N$  is the number of neurons.

The parity plot (Fig. 7) of the ANN for  $N_{s,a}$  with abscissa represents the numerically generated  $N_{s,a}$  and the ordinate represents  $N_{s,a}$  predicted by the neural network. As a majority of the data lie within 8% of the parity line, it can be concluded that the neural network developed in the present study is adequate to predict  $N_{s,a}$  and serves as surrogate to numerically developed value. Table 1 shows the variation of RMSE with a number of neurons in the hidden layer. From this study, a network with 4 neurons in the hidden layer with RMSE of 0.009 is selected.

Table 1: Number of neurons in hidden layer and RMSE.

Serial No.	No. of neurons	RMSE
1	2	0.013153
2	3	0.012692
3	4	0.009430
4	5	0.012550
5	6	0.012139
6	7	0.011900
7	8	0.018700
8	9	0.014290
9	10	0.015710

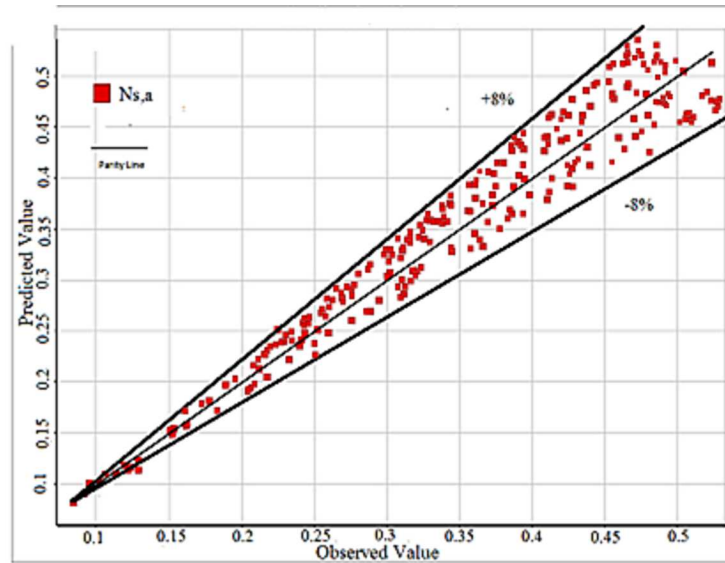


Figure 7: Partity plot showing the adequacy of the ANN.

#### 4.4 Optimization

The objective function is minimization of entropy augmentation generation number and may be assumed as  $N_{s,a} = f(D, W, L)$ . A total of 50 simulation results are fed into ANN by varying depth, width, and length within the considered range. After 51 generations GA yielded the optimum value and

for  $\mu$ GA, it is 52 generations. As heat transfer rate is augmented, with escalating surface area optimum, the value yielded is 0.137882 for genetic algorithm and 0.138352 for microgenetic algorithm (Tab. 2). By using the  $\mu$ GA the computational time is reduced more than half with significantly smaller variation in optimum values.

Table 2: Optimization results.

Algorithm	Re	Width (mm)	Depth (mm)	Length (mm)		Computational time (s)
GA	200	2.00362	4	8.1	0.2409	280
	300	2.1	4	8.02	0.193	270
	400	3	2	8	0.146	260
	500	2.386788	4	8	0.111	255
	600	2.32782	4	8	0.08	250
$\mu$ GA	200	2.23	3.87	8.15	0.22	60
	300	2.22	3.7	8.4	0.185	55
	400	2.8	2.3	8.2	0.133	40
	500	2.56	3.78	8.2	0.097	48
	600	2.7	3.7	8.4	0.092	39

## 5 Conclusions

Ribs on the duct surface have enhanced the heat transfer rate at the optimal cost of pressure drop. For the length, width, and depth of the rib, respectively 3 mm, 2 mm, and 8 mm the Nusselt number is increased from (5.1 to 9.2) at low Reynolds number in the laminar regime (200 to 600), whereas friction factor is decreased (from 0.4 to 0.24). Entropy augmentation generation number considered for the performance evaluation was decreased with increase in Reynolds number (200 to 600) from 0.5 to 0.1 for the above mentioned depth, width and length of rib. The trend is being similar for all configurations of ribs. It is been observed that the influence of depth of rib is more compared to others on entropy augmentation generation number.

Further optimization is carried for ribs of different dimensions placed alternatively on top and bottom of the surface using the artificial neural network combined with the genetic algorithm. Optimum conditions are

obtained as the Reynolds number varied from 100 to 600, length variation with Reynolds number is not significant to a great extent but the depth has a dip at Reynolds number of 400 with simultaneous increase in width. Value has decreased with increase in Reynolds number indicating augmentation of heat transfer. Then the results obtained with the genetic algorithm are compared with the microgenetic algorithm. Both of them gave the optimum conditions with variation less than 5% and the computational time was reduced by more than six times (for the Reynolds number 600 the computational time was 250 s for the case of genetic algorithm, while only 39 s for microgenetic algorithm) .

*Received 8 October 2018*

## References

- [1] THIANPONG C., EIAMSA-ARD P. , WONGCHAREE K., EIAMSA-ARD S.: *Compound heat transfer enhancement of a dimpled tube with a twisted tape swirl generator*. Int. Commun. Heat Mass Transf. **36**(2009), 7, 698–704.
- [2] KATHAIT P.S., PATIL A.K.: *Thermohydraulic performance of a heat exchanger tube with discrete corrugations*. Appl. Therm. Eng. **66**(2014), 1, 162–170.
- [3] KAMALI R., BINESH A.: *The importance of rib shape effects on the local heat transfer and flow friction characteristics of square ducts with ribbed internal surfaces*. Int. Commun. Heat Mass Transf. **35**(2008), 8, 1032–1040.
- [4] JAURKER A.R., SAINI J.S.: , GANDHI B.K.: *Heat transfer and friction characteristics of rectangular solar air heater duct using rib-grooved artificial roughness*. Sol. Energy **80**(2006), 8, 895–907.
- [5] THIANPONG C., CHOMPOOKHAM T., SKULLONG S., PROMVONGE P.: *Thermal characterization of turbulent flow in a channel with isosceles triangular*. Int. Commun. Heat Mass Transf. **36**(2009), 7, 712–717.
- [6] WEBB R.L., ECKERT E.R.G., GOLDSTEIN R.J.: *Heat transfer and friction in tubes with repeated-rib roughness*. Int. J. Heat Mass Tran. **14**(1971), 4, 601–617.
- [7] MANCA O., NARDINI S., RICCI D.: *Numerical study of air forced convection in a rectangular channel provided with ribs*. In: Proc. 14th Int. Heat Transfer Conf. ASME (IHTC14), Washington D.C., 8-13 Aug. 2010, 861-870.
- [8] THIANPONG C., CHOMPOOKHAM T., SKULLONG S., PROMVONGE P.: *Thermal characterization of turbulent flow in a channel with isosceles triangular*. Int. Commun. Heat Mass Transf. **36**(2009), 712–717.
- [9] SKULLONG S. , CHAIDILOKPATTANAKUL P. , PROMVONGE P.: *Effect of inclined ribs on heat transfer behavior in a square channel*. In: Proc. 11th Int. Conf. Utility Exhib. on Power and Energy Systems: Issues and Prospects for Asia (ICUE 2011), Pattaya , 28-30 Sep., 2011, 1–5.

- [10] CHOI E.Y., YONG D.C., LEE W.S., JIN T.C., KWAK J.S.: *Heat Transfer augmentation using a rib-dimple compound cooling technique*. *Appl. Therm. Eng.* **51**(2013), 1-2, 435–441.
- [11] LIU J., XIE G., SUNDEN B., WANG L., ANDERSSON M.: *Enhancement of heat transfer in a square channel by roughened surfaces in rib-elements and turbulent flow manipulation*. *Int. J. Numer. Method. Heat Fluid Flow* **27**(2017),7, 1571–1595.
- [12] ABED A.M., SOPIAN K., MOHAMMED H., ALGHOUL M., RUSLAN M.H., MAT S., ALI NAJAH AL-SHAMANI: *Enhance heat transfer in the channel with V-shaped wavy lower plate using liquid nano fluids*. *Case Stud. Therm. Eng.* **5**(2015), 13–23.
- [13] PIECHOWSKI M.: *A Ground Coupled Heat Pump System with Energy Storage*. PhD thesis, University of Melbourne, Melbourne 1996.
- [14] BEJAN A.V.: *The concept of irreversibility in heat exchanger design: counterflow heat exchangers for gas-to-gas application*. *J. Heat. Trans.* **99**(1977) 3, 374–80.
- [15] BEJAN A.: *General criterion for rating heat-exchanger performance*. *Int. J. Heat Mass Transf.* **21**(1978), 5, 655–8.
- [16] BEJAN A.: *A study of entropy generation in fundamental convective heat transfer*. *J. Heat Trans.* **101**(1979), 4, 718–25.
- [17] BEJAN A.: *Second-law analysis in heat transfer*. *Energy* **5**(1980), 8, 721–732.
- [18] SEKULIC D.P.: *Entropy generation in a heat exchanger*: *Heat Transfer Eng.* **7**(1986), 1-2, 83–88.
- [19] SEKULIC D.P.: *The second law quality of energy transformation in a heat exchanger*. *J. Heat Trans.* **112**(1990), 2, 295–300.
- [20] OGULATA R.T., DOBA F., YILMAZ T.: *Irreversibility analysis of cross flow heat exchangers*. *Energ. Convers. Manag.* **41**(2000), 15, 1585–99.
- [21] LASKOWSKI R., RUSOWICZ A., GRZEBIELEC A.: *Estimation of a tube diameter in a 'church window' condenser based on entropy generation minimization*. *Arch. Thermodyn.* **36**(2015), 3, 49–59.
- [22] KONCHADA P., PV V., BHEMUNI V.: *Statistical analysis of entropy generation in longitudinally finned tube heat exchanger with shell side nanofluid by a single phase approach*. *Arch. Thermodyn.* **37**(2016), 2, 3–22.
- [23] KADIYALA P.K., CHATTOPADHYAY H.: *Optimal location of three heat sources on the wall of a square cavity using genetic algorithms integrated with artificial neural networks*. *Int. Commun. Heat Mass Transf.* **38**(2011), 5, 620–624.
- [24] KADIYALA P.K., CHATTOPADHYAY H.: *Neuro-genetic optimization of laminar slot jets impinging on a moving surface*. *Int. Commun. Heat Mass Transf.* **59**(2014), 143–147.
- [25] LI W., KHAN T., TANG W., MINKOWYCZ W.J.: *Numerical study and optimization of corrugation height and angle of attack of vortex generator in the wavy fin-and-tube heat exchanger*. *J. Heat Trans.* **140**(2018), 11, 111801-1–111801-11.
- [26] GE Y., WANG S.C., LIU Z.C., LIU W.: *Optimal shape design of a minichannel heat sink applying multi-objective optimization algorithm and three-dimensional numerical method*. *Appl. Therm. Eng.* **148**(2019), 120–128.

- 
- [27] KISHORE P.S., KOTESWARA REDDY V., PREM DHEERAJ M., PAVAN KUMAR K.: *Study and optimization of parameters that influence thermohydraulic performance of flow in a duct with twisted tape insert in conjunction with dimples over its surface.* J. Enhanc. Heat Transf. **23**(2016), 6, 499–512.
- [28] SAHA S.K., MALIK S.K.: *Heat transfer and pressure drop characteristics of laminar flow in rectangular and square plain ducts and ducts with twisted-tape inserts.* J. Heat Trans. **127**(2005), 9, 966–977.
- [29] BEJAN A., PFISTER P.A. JR: *Evaluation of heat transfer augmentation techniques based on their impact on entropy generation.* Lett. Heat Mass Trans. **7**(1980), 2, 97–106.
- [30] BEJAN A.: *Entropy Generation through Heat and Fluid Flow*, Wiley, New York 1982.
- [31] HESSELGREAVES J.E.: *Rationalisation of second law analysis of heat exchangers.* Int. J. Heat Mass Tran. **43**(2000), 22, 4189–4204.
- [32] ZIMPAROV V.: *Extended performance evaluation criteria for enhanced heat transfer surfaces: heat transfer through ducts with constant heat flux.* Int. J. Heat Mass Tran. **44**(2001), 1, 169–180.
- [33] GOLDBERG D.E.: *Genetic Algorithms in Search, Optimization, and Machine Learning.* Addison-Wesley, Reading 1989.
- [34] WHITLEY D.: *A Genetic Algorithm Tutorial.* Colorado State University, Techn. Rep. CS-93-103, 1993.
- [35] MADADI R.R., BALAJI C.: *Optimization of the location of multiple discrete heat sources in a ventilated cavity using artificial neural networks and micro genetic algorithm.* Int. J. Heat Mass Transf. **51**(2008), 9-10, 2299–2312.
- [36] NONINO C., COMINI G.: *Convective heat transfer in ribbed square channels.* Int. J. Numer. Method. Heat Fluid Flow **12**(2002), 5, 610–628.